IEEE Access
Multidisciplinary | Rapid Review | Open Access Journal

Received October 29, 2019, accepted November 21, 2019, date of publication November 27, 2019,
date of current version December 11, 2019.

Digital Object Identifier 10.1109/ACCESS.2019.2956188

Adaptive Nonsingular Terminal Sliding Mode Backstepping Control for the Speed and Tension System of the Reversible Cold Strip Rolling Mill Using Disturbance Observers

LE LIU[1], SUYAN DING[1], JIE GAO[1], AND YIMING FANG[1,2]
[1]College of Electrical Engineering, Yanshan University, Qinhuangdao 066004, China
[2]National Engineering Research Center for Equipment and Technology of Cold Strip Rolling, Qinhuangdao 066004, China

Corresponding author: Le Liu (leliu@ysu.edu.cn)

This work was supported in part by the National Natural Science Foundation of China under Grant 61803327, in part by the Natural Science Foundation of Hebei Province under Grant F2016203263, in part by the Research Foundation of Hebei University of Environmental Engineering under Grant BJ201604, in part by the Key Research and Development Project of Hebei Province under Grant 18212109, and in part by the Basic Research Specific Subject of Yanshan University under Grant 16LGA005.

ABSTRACT In order to weaken the influences of system uncertainties and coupling items on the coordinated tracking control performance of the speed and tension system of the reversible cold strip rolling mill, an adaptive nonsingular terminal sliding mode (ANTSM) backstepping control strategy using disturbance observers is proposed. First, time-varying gain extended state observers (TVGESOs) are constructed to dynamically observe the system's mismatched uncertainties, which weaken the initial peak phenomenon of the traditional extended state observer (ESO), and effectively improve the system's tracking control precision. Next, based on the backstepping control and the second order sliding mode integral filters, adaptive nonsingular terminal sliding mode controllers (ANTSMCs) for the speed and tension system of the reversible cold strip rolling mill are designed, which solve the ''differential explosion'' problem of conventional backstepping control, and make sliding mode variables converge in finite time. Again, neural network adaptive method is used to approximate the system's matched uncertainties, and the approximation values are introduced into the designed controllers for compensations. Finally, simulation research is carried out on the speed and tension system of a 1422 mm reversible cold strip rolling mill by using actual data, and the results show the validity of the proposed control strategy.

INDEX TERMS Reversing cold strip rolling mill, speed and tension system, time-varying gain extended state observer (TVGESO), adaptive nonsingular terminal sliding mode control (ANTSMC), backstepping control, second order sliding mode integral filter.

I. INTRODUCTION

Reversible cold strip rolling mill is the exclusive equipment for producing strip steel products, such as special steel, ordinary carbon steel, low-alloy steel, and so on [1]. Maintaining constant tension is essential to guaranteeing the strip steel product quality, and making the rolling process run smoothly. This is because the strip steel tension not only reduces the metal deformation resistance and deformation work, decreases the energy consumption, and prevents the rolled piece running away, but also makes the rolled piece elongate uniformly in both horizontal and vertical directions [2]. Besides, when the hard and (extremely) thin strip steel is rolled, the roller might be hard to have any rolling effects on the strip steel thickness because of the elastic deformation, but the expected shape and thickness of strip steel can be obtained by adjusting the strip steel tension [3].

Actually, in the production process of the cold strip rolling mill, the left coiler, the main rolling mill, and the right coiler are flexibly connected through the strip steel. They constitute a complex time-varying system that is multivariate, is nonlinear, has strong coupling, and is uncertain [4].

The associate editor coordinating the review of this manuscript and approving it for publication was Jianyong Yao.

Conventional control strategies, whether feedforward control or feedback control, mostly use the single variable control principle [5], that is, the coupling between the speed and tension is artificially ignored, and the speed control system and the tension control system are individually designed. This cognitive limitation restricts further improvement of the strip steel product quality.

In order to realize decoupling and coordinated tracking control for the speed and tension system of the cold strip rolling mill, relevant control strategies have been proposed by many scholars. Liu *et al*. [6] used the ESO to observe the system states and the total uncertainty, which improved the system's control precision. However, the selected constant observer gain cannot guarantee the observation precision of ESO, and when the initial state value of ESO is not equal to the real initial state value, the high gain may cause initial peak phenomenon of the observation value of uncertainty. Yao *et al.* [7]–[9] adopted the robust integral of the sign of the error (RISE) control strategy to suppress the modeling uncertainties, which ensured the asymptotic stability despite of the existence of unstructured uncertainties, and obtained high-accuracy tracking control of systems greatly. Liu *et al.* [10] proposed a decentralized overlapping control method based on the inclusion principle, which realized coordinated control among the left coiler tension, the main rolling mill speed, and the right coiler tension. While the calculation process of this controller design method was relatively complicated. Bai *et al.* [11] completed the controller design based on the pole assignment method, which weakened the coupling and effectively improved the system's dynamic and static performance. While this controller design method had a relatively high requirement on the system model precision. Fang *et al*. [12] proposed a nonsingular fast terminal sliding mode control strategy, which improved the global convergence speed and the robust stability of the system. However, the system's control precision and dynamic performance are closely related to the sliding mode surface parameters, that is, if the parameters are not properly selected, potential chatter and undesired dynamic performance may be activated. Koc *et al*. [13] designed the H_∞ robust controller for each main channel to improve the system's anti-interference ability. Yet this controller design method had relatively strong conservatism. Fang *et al*. [14] proposed a compound control method based on the invariance principle. This method required the virtual control variables to be differentiated repeatedly in the backstepping design process, which made the complexities of the designed controllers grow dramatically with the increase of system relative order. In other words, this design was prone to causing ''differential explosion'' problem.

While in each step of backstepping control, the second order sliding mode integral filter [15], [16] could estimate the derivative of the virtual control variable, which can not only avoid the ''differential explosion'' problem, and simplify the system controller's design process, but also filter out the measurement noise, and reduce the estimation error of the filter and ensure its fast convergence. Further, by adjusting the observer gain from small to large, the TVGESO [17] can effectively reduce the initial peak phenomenon of the traditional ESO, which is beneficial to improve the system's control precision. The ANTSM control method [18] timely and accurately updates the sliding mode surface parameters through the adaptive function, which can smooth the system trajectory, and effectively improve the system's robust stability and control precision. In addition, the RBF neural network [19]–[22] has the advantage of a strong learning ability, and is often used to approximate arbitrary complex nonlinear functions in the nonlinear control field.

Based on the above analysis, this paper proposes an ANTSM backstepping control strategy for the speed and tension system of the reversible cold strip rolling mill using TVGESOs. First, the system's unmatched uncertainties are observed by constructing TVGESOs. Second, ANTSMCs for the speed and tension system of the reversible cold strip rolling mill are designed based on the backstepping control and the second order sliding mode integral filters. Third, the RBF neural networks are adopted to approximate the system's matched uncertainties. Finally, simulation research is carried out on the speed and tension system of a 1422 mm reversible cold strip rolling mill by using actual data, and the results show that the proposed control strategy can not only improve the coordinated tracking control performance of the system, but also has better dynamic and static performance and robust stability.

The main contributions of this paper are summarized as follows:

(1) The TVGESOs are constructed to dynamically observe the unmatched uncertainties, which weaken the initial peak phenomenon of traditional ESO, and improve the system's control precision effectively.

(2) The ANTSMCs are designed based on the backstepping control and the second order sliding mode integral filters, which avoid the ''differential explosion'' phenomena in backstepping process, improve the system's robust stability, and make the sliding mode variables converge in finite time.

(3) The neural networks are developed, which dynamically approximate the matched uncertainties, and improve the system's stability precision effectively.

The remainder of this paper is organized as follows: In section II, the system model is described and the control problems are formulated. In section III, the design process of the TVGESOs are presented. In section IV, the ANTSMCs are designed, and the neural network adaptive method is adopted to approximate the matched uncertainties. In section V, the stability and convergence analyses are given. In section VI, the simulation research is presented to illustrate the validity of the proposed control strategy. The conclusion is given in section VII.

II. SYSTEM DESCRIPTION AND CONTROL PROBLEM FORMULATION

A. SYSTEM DESCRIPTION

The reversible cold strip rolling mill is mainly composed of left coiler, main rolling mill, right coiler, guide rollers, and so on. The structure diagram of the reversible cold strip rolling mill is shown as Fig. 1.

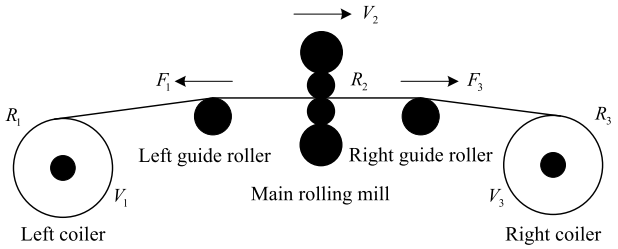

FIGURE 1. Structure diagram of the reversible cold strip rolling mill.

According to related rolling theory and the dynamic equations of the DC motor, the mathematic model for the speed and tension system of the reversible cold strip rolling mill is described as follows [23]:

$$\text{sys}_1:\begin{cases}\dot{F}_1=\dfrac{EA_1}{L}\left[V_2\left(1-\chi_0\left(1+K_\chi F_1\right)\right)-V_1\right]\\ \dot{V}_1=\dfrac{K_1R_1}{J_1\eta_1}I_1+\dfrac{R_1^2}{J_1\eta_1^2}F_1-\left(\dfrac{B_{u1}}{J_1}-\dfrac{\dot{R}_1}{R_1}\right)V_1\\ \dot{I}_1=\dfrac{K_{s1}}{l_1}u_1-\dfrac{K_1\eta_1}{l_1R_1}V_1-\dfrac{r_1}{l_1}I_1\\ \dot{J}_1\left(t\right)=\dfrac{2\pi\rho B}{\eta_1^2}R_1^3\dot{R}_1,\ \dot{R}_1=-\dfrac{H}{2\pi R_1}V_1\end{cases}\tag{1a}$$

$$\text{sys}_2:\begin{cases}\dot{V}_2=\dfrac{K_2R_2}{J_2\eta_2}I_2+\dfrac{R_2^2}{J_2\eta_2^2}\left(F_3-F_1\right)\\ -\dfrac{B_{u2}}{J_2}V_2-\dfrac{M_zR_2}{J_2\eta_2^2}\\ \dot{I}_2=\dfrac{K_{s2}}{l_2}u_2-\dfrac{K_2\eta_2}{l_2R_2}V_2-\dfrac{r_2}{l_2}I_2\end{cases}\tag{1b}$$

$$\text{sys}_3:\begin{cases}\dot{F}_3=\dfrac{EA_2}{L}\left[V_3-V_2\left(1+\delta_0\left(1+K_\delta F_3\right)\right)\right]\\ \dot{V}_3=\dfrac{K_3R_3}{J_3\eta_3}I_3-\dfrac{R_3^2}{J_3\eta_3^2}F_3-\left(\dfrac{B_{u3}}{J_3}-\dfrac{\dot{R}_3}{R_3}\right)V_3\\ \dot{I}_3=\dfrac{K_{s3}}{l_3}u_3-\dfrac{K_3\eta_3}{l_3R_3}V_3-\dfrac{r_3}{l_3}I_3\\ \dot{J}_3\left(t\right)=\dfrac{2\pi\rho B}{\eta_3^2}R_3^3\dot{R}_3,\ \dot{R}_3\left(t\right)=\dfrac{h}{2\pi R_3}V_3\end{cases}\tag{1c}$$

where sys_1 is the left coiler tension subsystem, sys_2 is the main rolling mill speed subsystem, and sys_3 is the right coiler tension subsystem. K_i is the torque coefficient; $J_i \in \mathrm{R}^3$ is the rotational inertia; $V_i \in \mathrm{R}^3$ is the linear velocity; η_i is the reduction ratio; $B_{ui} \in \mathrm{R}^3$ is the friction coefficient; $u_i \in \mathrm{R}^3$ and Ks_i are the control voltage and amplification of the rectifying device in a DC motor, respectively; $I_i,\ r_i \in \mathrm{R}^3$, and l_i are the current, resistance and inductance of the armature circuit, respectively; R_1 and R_3 are the steel coil radii of the left and right coilers, respectively; R_2 is the work roll radius of the main rolling mill; E is elastic modulus; B, ρ, H, and h are the width, density, inlet thickness and outlet thickness of strip steel, respectively; $F_1,\ F_3 \in \mathrm{R}$, and A_1, A_2 are the strip steel tensions and crosscut areas on both sides of the main rolling mill, respectively; $M_z \in \mathrm{R}$ is the rolling torque; δ_0 and χ_0 are the forward and backward slip coefficients without tension, respectively; K_δ and K_χ are the impact factors that tension adds to the forward and backward slip coefficients, respectively.

Remark 1: $i = 1, 2, 3$ are the subscripts, which indicate the parameters belong to the subsystems sys_1, sys_2, and sys_3, respectively.

The steel coil radii (R_1, R_3) and the rotational inertias (J_1, J_3) of the coilers are slow time-varying parameters, and for the convenience of research, $(R_1,\ R_3,\ J_1,\ J_3)$ were replaced with the median values $\left(\bar{R}_1,\ \bar{R}_3,\ \bar{J}_1,\ \bar{J}_3\right)$, and then $\dot{\bar{R}}_1 = \dot{\bar{R}}_3 = \dot{\bar{J}}_1 = \dot{\bar{J}}_3 = 0$. In addition, considering the perturbations of the friction coefficient B_{ui} and the armature resistance r_i, as well as the load disturbance ΔM_z, then the speed and tension system model (1) of the reversible cold strip rolling mill can be equivalently converted as

$$\text{sys'}_1:\begin{cases}\dot{F}_1=\dfrac{EA_1}{L}\left[V_2\left(1-\chi_0\left(1+K_\chi F_1\right)\right)-V_1\right]\\ \dot{V}_1=\dfrac{K_1\bar{R}_1}{\bar{J}_1\eta_1}I_1+\dfrac{\bar{R}_1^2}{\bar{J}_1\eta_1^2}F_1-\dfrac{B_{u1}}{\bar{J}_1}V_1+\Delta_1\\ \dot{I}_1=\dfrac{K_{s1}}{l_1}u_1-\dfrac{K_1\eta_1}{l_1\bar{R}_1}V_1-\dfrac{r_1}{l_1}I_1+\omega_1\end{cases}\tag{2a}$$

$$\text{sys'}_2:\begin{cases}\dot{V}_2=\dfrac{K_2R_2}{J_2\eta_2}I_2+\dfrac{R_2^2}{J_2\eta_2^2}\left(F_3-F_1\right)\\ -\dfrac{B_{u2}}{J_2}V_2-\dfrac{M_zR_2}{J_2\eta_2^2}+\Delta_2\\ \dot{I}_2=\dfrac{K_{s2}}{l_2}u_2-\dfrac{K_2\eta_2}{l_2R_2}V_2-\dfrac{r_2}{l_2}I_2+\omega_2\end{cases}\tag{2b}$$

$$\text{sys'}_3:\begin{cases}\dot{F}_3=\dfrac{EA_2}{L}\left[V_3-V_2\left(1+\delta_0\left(1+K_\delta F_3\right)\right)\right]\\ \dot{V}_3=\dfrac{K_3\bar{R}_3}{\bar{J}_3\eta_3}I_3-\dfrac{\bar{R}_3^2}{\bar{J}_3\eta_3^2}F_3-\dfrac{B_{u3}}{\bar{J}_3}V_3+\Delta_3\\ \dot{I}_3=\dfrac{K_{s3}}{l_3}u_3-\dfrac{K_3\eta_3}{l_3\bar{R}_3}V_3-\dfrac{r_3}{l_3}I_3+\omega_3\end{cases}\tag{2c}$$

where Δ_i and ω_i are the system's unmatched uncertainty and matched uncertainty, respectively.

B. CONTROL PROBLEM FORMULATION.

The goal of this paper is to realize coordinated tracking control for the target values of the system, that is, $F_1 \to F_1^*$, $V_2 \to V_2^*$, and $F_3 \to F_3^*$. However, as can be clearly seen in the system model (2), there exists coupling between the speed and tension of the reversible cold strip rolling mill, and the rolling mill system (2) simultaneously suffers the influences of the unmatched uncertainty Δ_i and the matched uncertainty ω_i. Therefore, from the perspective of control theory, the control problems for the rolling mill system (2) can be formulated as follows:

1) Construct observer to realize dynamic observation for the unmatched uncertainty Δ_i in the speed and tension system (2).

2) Design controllers $\boldsymbol{u}$ to improve the system's robust stability, weaken the influences of system coupling items, and realize coordinated tracking control for the system given values F_1^*, V_2^*, and F_3^*.

3) Approximate the matched uncertainty ω_i in the speed and tension system (2), and the approximation values are introduced into the designed controllers $\boldsymbol{u}$ for compensations.

III. CONSTRUCTIONS OF TIME-VARYING GAIN EXTENDED STATE OBSERVERS (TVGESOs) FOR THE MISMATCHED UNCERTAINTIES

The conventional ESO is a nonlinear state observer consisting of a set of nonlinear functions. It can not only reproduce the state variables of the control object, but also take the internal and external disturbances of the n-order system as the $n+1$ state and observe it. However, for uncertainty with an unknown upper bound, the selection of constant observer gain cannot guarantee the estimation precision of ESO, and the initial peak phenomenon caused by high gain easily leads to system instability. For this problem, a novel TVGESO is constructed to observe the unmatched uncertainty Δ_i in this section, and the proof process of its stability is also given.

Assumption 1: The first derivative of the unmatched uncertainty Δ_i is bounded, that is, there exists an unknown positive μ_i, which makes $\left|\dot{\Delta}_i\right| \leq \mu_i$ hold.

Then based on (2), the TVGESOs can be respectively constructed as

$$\mathrm{TVGESO}_1: \begin{cases} \sigma_{11} = z_{11} - V_1 \\ \dot{z}_{11} = \dfrac{K_1\bar{R}_1}{\bar{J}_1\eta_1} I_1 + \dfrac{\bar{R}_1^2}{\bar{J}_1\eta_1^2} F_1 - \dfrac{B_{u1}}{\bar{J}_1} z_{11} \\ \quad + z_{12} - l_{11}(t)(z_{11} - V_1) \\ \dot{z}_{12} = -l_{12}(t)(z_{11} - V_1) \end{cases} \tag{3a}$$

$$\mathrm{TVGESO}_2: \begin{cases} \sigma_{21} = z_{21} - V_2 \\ \dot{z}_{21} = \dfrac{K_2R_2}{J_2\eta_2} I_2 + \dfrac{R_2^2}{J_2\eta_2^2}(F_3 - F_1) + z_{22} \\ \quad - \dfrac{M_Z R_2}{J_2\eta_2^2} - \dfrac{B_{u2}}{J_2} z_{21} - l_{21}(t)(z_{21} - V_2) \\ \dot{z}_{22} = -l_{22}(t)(z_{21} - V_2) \end{cases} \tag{3b}$$

$$\mathrm{TVGESO}_3: \begin{cases} \sigma_{31} = z_{31} - V_3 \\ \dot{z}_{31} = \dfrac{K_3\bar{R}_3}{\bar{J}_3\eta_3} I_3 - \dfrac{\bar{R}_3^2}{\bar{J}_3\eta_3^2} F_3 - \dfrac{B_{u3}}{\bar{J}_3} z_{31} \\ \quad + z_{32} - l_{31}(t)(z_{31} - V_3) \\ \dot{z}_{32} = -l_{32}(t)(z_{31} - V_3) \end{cases} \tag{3c}$$

where z_{i1} is the observation value of V_i, and σ_{i1} is the observation error; z_{i2} is the observation value of Δ_i; l_{i1} and l_{i2} are the time-varying gains, which can be designed as

$$l_{i1}(t) = 2L_i(t),\ l_{i2}(t) = L_i^2(t) \tag{4}$$

where $L_i(t)$ is an adaptive update function with the following form:

$$\dot{L}_i(t) = \begin{cases} \varsigma_i |\sigma_{i1}| & L_i(t) \leq L_{i\max} \text{ and } |\sigma_{i1}| > \varphi_i \\ 0 & \text{others} \end{cases} \tag{5}$$

where $L_{i\max} \in \mathrm{R}^+$ stands for the maximum value of $L_i(t)$, $\varphi_i \in \mathrm{R}^+$ is the dead zone bound, and $\varsigma_i \in \mathrm{R}^+$ is the adaptive parameter.

Define the observation error as

$$\sigma_{i2} = z_{i2} - \Delta_i \tag{6}$$

Theorem 1: For the unmatched uncertainty Δ_i in the system model (2), the constructed TVGESOs can guarantee that the observation errors are bounded, and their upper bounds depend on the adaptive update function $L_i(t)$.

Proof: For simplicity, take the main rolling mill speed subsystem sys'$_2$ as an example.

First, according to the main rolling mill speed subsystem (2b) and the constructed TVGESO$_2$ (3b), the dynamic equations of the observation errors are

$$\begin{cases} \dot{\sigma}_{21} = -\left(l_{21} + \dfrac{B_{u2}}{J_2}\right)\sigma_{21}(t) + \sigma_{22}(t) \\ \dot{\sigma}_{22} = -l_{22}\sigma_{21}(t) - \dot{\Delta}_2 \end{cases} \tag{7}$$

Define $X_1 = \sigma_{21}(t)$, $X_2 = \sigma_{22}(t) - \left(l_{21} + \frac{B_{u2}}{J_2}\right)\sigma_{21}(t)$, and their differential equations are

$$\begin{cases} \dot{X}_1 = X_2 \\ \dot{X}_2 = -\left(\dot{l}_{21} + l_{22}\right)X_1 - \left(l_{21} + \dfrac{B_{u2}}{J_2}\right)X_2 - \dot{\Delta}_2 \end{cases} \tag{8}$$

Choose the Lyapunov function candidate as

$$V_1 = \int_0^{X_1} \left(\dot{l}_{21} + l_{22}\right) X_1(\tau) dX_1(\tau) + \frac{X_2^2}{2} \tag{9}$$

and the time derivative of V_1 is

$$\begin{aligned} \dot{V}_1 &= \left(\dot{l}_{21} + l_{22}\right)X_1X_2 + X_2\dot{X}_2 \\ &= \left(\dot{l}_{21} + l_{22}\right)X_1X_2 + X_2\left(-\left(\dot{l}_{21} + l_{22}\right)X_1 \right. \\ &\quad \left. - \left(l_{21} + \frac{B_{u2}}{J_2}\right)X_2 - \dot{\Delta}_2\right) \\ &= -\left(l_{21} + \frac{B_{u2}}{J_2}\right)X_2^2 - \dot{\Delta}_2X_2 \\ &\leq -\left(l_{21} + \frac{B_{u2}}{J_2}\right)X_2^2 + \left|\dot{\Delta}_2\right||X_2| \\ &\leq -C|X_2|^2 \end{aligned} \tag{10}$$

where $C = l_{21} + \frac{B_{u2}}{J_2} - \frac{\mu_2}{|X_2|}$.

Under the condition that $C > 0$, i.e. $|X_2| > \frac{\mu_2}{l_{21} + \frac{B_{u2}}{J_2}}$, and we have

$$\dot{V}_1 < 0 \tag{11}$$

Then we can get the constructed TVGESO$_2$ (3b) is stable, and the state trajectory will converge to the following bound [24], [28]:

$$|X_2| \leq \frac{\mu_2}{l_{21} + \frac{B_{u2}}{J_2}} \tag{12}$$

Further, when the state reaches stability, there is

$$\dot{X}_2 = -\left(\dot{l}_{21} + l_{22}\right) X_1 - \left(l_{21} + \frac{B_{u2}}{J_2}\right) X_2 - \dot{\Delta}_2 = 0 \tag{13}$$

Then take the absolute value of the (13), and the following can be obtained:

$$\begin{aligned} |X_1| = |\sigma_{21}(t)| &= \left|\dot{\Delta}_2 + \left(l_{21} + \frac{B_{u2}}{J_2}\right) X_2\right| \Big/ \left|\dot{l}_{21} + l_{22}\right| \\ &\leq \left(\left|\dot{\Delta}_2\right| + \left|\left(l_{21} + \frac{B_{u2}}{J_2}\right) \frac{\mu_2}{l_{21} + \frac{B_{u2}}{J_2}}\right|\right) \Big/ \left|\dot{l}_{21} + l_{22}\right| \\ &\leq 2\mu_2 \Big/ L_2^2 \end{aligned} \tag{14}$$

By (12) and (14), we can get

$$\begin{aligned} |\sigma_{22}(t)| &= \left|\left(l_{21} + \frac{B_{u2}}{J_2}\right) \sigma_{21}(t) + X_2\right| \\ &\leq \left(l_{21} + \frac{B_{u2}}{J_2}\right) |X_1| + |X_2| \\ &\leq \left(2L_2 + \frac{B_{u2}}{J_2}\right) \frac{2\mu_2}{L_2^2} + \frac{\mu_2}{2L_2 + \frac{B_{u2}}{J_2}} \\ &\leq \left(\frac{9}{2} + \frac{2B_{u2}}{J_2 L_2}\right) \frac{\mu_2}{L_2} \end{aligned} \tag{15}$$

Since $L_2(t)$ is an increasing function, then the bounds of the two observation errors satisfy

$$\begin{cases} |\sigma_{21}| \leq 2\mu_2 \Big/ L_{2\min}^2 \\ |\sigma_{22}| \leq \left(\dfrac{9}{2} + \dfrac{2B_{u2}}{J_2 L_{2\min}}\right) \dfrac{\mu_2}{L_{2\min}} \end{cases} \tag{16}$$

where $L_{2\min} \in \mathrm{R}^+$ stands for the minimum value of $L_2(t)$.

By (16), it can be concluded that the observation errors σ_{21} and σ_{22} are bounded, and their upper bounds depend on the adaptive update function $L_2(t)$.

IV. CONTROLLER DESIGNS FOR THE SPEED AND TENSION SYSTEM OF THE REVERSIBLE COLD STRIP ROLLING MILL

In this section, combined with the backstepping control and the second order sliding mode integral filters, the ANTSMCs are designed to improve the global convergence speed of the system, suppress the potential chatter and undesired dynamic performance, and avoid the ''differential explosion'' problem in the backstepping design process. Besides, the RBF neural network adaptive method is adopted to approximate the system's matched uncertainty ω_i, so as to improve the tracking control precision of the system.

A. DESIGNS OF ADAPTIVE NONSINGULAR TERMINAL SLIDING MODE CONTROLLERS (ANTSMCs)

Based on system (2), the controllers for the speed and tension system of the reversible cold strip rolling mill are designed as follows:

Firstly, we start with the left coiler tension subsystem sys'$_1$.

Step 1: By (2a), the tracking error of the left coiler tension is defined as $e_{11} = F_1 - F_1^*$, and the time derivative of e_{11} is

$$\dot{e}_{11} = \frac{EA_1}{L}\left[V_2\left(1 - \chi_0\left(1 + k_\chi F_1\right)\right) - V_1\right] - \dot{F}_1^* \tag{17}$$

where F_1^* is the given value of the left coiler tension subsystem sys'$_1$.

Choose the Lyapunov function candidate as $V_{11} = \frac{1}{2}e_{11}^2$, and the time derivative of V_{11} is

$$\dot{V}_{11} = e_{11}\left(\frac{EA_1}{L}\left[V_2\left(1 - \chi_0\left(1 + k_\chi F_1\right)\right) - V_1\right] - \dot{F}_1^*\right) \tag{18}$$

By (18), the first virtual control variable V_{1d} can be designed as

$$V_{1d} = V_2\left(1 - \chi_0\left(1 + k_\chi F_1\right)\right) - \frac{L}{EA_1}\dot{F}_1^* + \frac{L}{EA_1}k_{11}e_{11} \tag{19}$$

where $k_{11} \in \mathrm{R}^+$ is the control parameter.

Step 2: Introduce an error variable $e_{12} = V_1 - V_{1d}$, and substitute e_{12} into (18) yields

$$\dot{V}_{11} = -k_{11}e_{11}^2 - \frac{EA_1}{L}e_{11}e_{12} \tag{20}$$

Choose the Lyapunov function candidate as $V_{12} = V_{11} + \frac{1}{2}e_{12}^2$, and the time derivative of V_{12} is

$$\begin{aligned} \dot{V}_{12} = -k_{11}e_{11}^2 - \frac{EA_1}{L}e_{11}e_{12} + e_{12}\Bigg(&\frac{K_1\bar{R}_1}{\bar{J}_1\eta_1}I_1 \\ &+ \frac{\bar{R}_1^2}{\bar{J}_1\eta_1^2}F_1 - \frac{B_{u1}}{\bar{J}_1}V_1 + \Delta_1 - \dot{V}_{1d}\Bigg) \end{aligned} \tag{21}$$

By (21), the second virtual control variable I_{1d} can be designed as

$$\begin{aligned} I_{1d} = \frac{\bar{J}_1\eta_1}{K_1\bar{R}_1}\Bigg(&-\frac{\bar{R}_1^2}{\bar{J}_1\eta_1^2}F_1 + \frac{B_{u1}}{\bar{J}_1}V_1 - z_{12} + \dot{V}_{1d} \\ &- k_{12}e_{12} - \hat{\rho}_{11}\mathrm{sign}(e_{12}) + \frac{EA_1}{L}e_{11}\Bigg) \end{aligned} \tag{22}$$

where $k_{12} \in \mathrm{R}^+$ is the control parameter; $\hat{\rho}_{11}$ is the estimation value of ρ_{11}, and the adaptive law can be designed as

$$\dot{\hat{\rho}}_{11} = \xi_{11}\left(|e_{12}| - \psi_{11}\hat{\rho}_{11}\right) \tag{23}$$

where ξ_{11}, $\psi_{11} \in \mathrm{R}^+$ are the adaptive control parameters, and the estimation error can be defined as $\tilde{\rho}_{11} = \rho_{11} - \hat{\rho}_{11}$.

In addition, in order to avoid the "differential explosion" problem in the backstepping process, we adopt a second order sliding mode integral filter to estimate $\dot{V}_{1d}$ in (22):

$$\begin{cases} \dot{\lambda}_{11} = -\dfrac{\lambda_{11} - V_{1d}}{\tau_{11}} - \dfrac{\gamma_{11}\left(\lambda_{11} - V_{1d}\right)}{\left|\lambda_{11} - V_{1d}\right| + \varepsilon_{11}} \\ \dot{\lambda}_{12} = -\dfrac{\lambda_{12} - \dot{\lambda}_{11}}{\tau_{12}} - \dfrac{\gamma_{12}\left(\lambda_{12} - \dot{\lambda}_{11}\right)}{\left|\lambda_{12} - \dot{\lambda}_{11}\right| + \varepsilon_{12}} \end{cases} \tag{24}$$

where λ_{11} and λ_{12} are the estimation values of V_{1d} and $\dot{V}_{1d}$, respectively. $\tau_{11},\ \tau_{12} \in \mathrm{R}^+$ are the time constants of the filter; $\gamma_{11},\ \gamma_{12},\ \varepsilon_{11},\ \varepsilon_{12} \in \mathrm{R}^+$ are the designed parameters.

Define the estimation error of the adopted second order sliding mode integral filter as $E_{12} = \lambda_{12} - \dot{V}_{1d}$, and we assume E_{12} is bounded, that is, $|E_{12}| \le \rho_{12}$, in which $\rho_{12} \in \mathrm{R}^+$ is the upper bound of E_{12}.

Then (22) can be redesigned as

$$\begin{aligned} I_{1d} = \frac{\bar{J}_1\eta_1}{K_1\bar{R}_1}\Bigg(&-\frac{\bar{R}_1^2}{\bar{J}_1\eta_1^2}F_1 + \frac{B_{u1}}{\bar{J}_1}V_1 - z_{12} + \lambda_{12} - k_{12}e_{12} \\ &- \hat{\rho}_{11}\mathrm{sign}(e_{12}) - \hat{\rho}_{12}\mathrm{sign}(e_{12}) + \frac{EA_1}{L}e_{11}\Bigg) \end{aligned} \tag{25}$$

where $\hat{\rho}_{12}$ is the estimation values of ρ_{12}, and the adaptive law can be designed as

$$\dot{\hat{\rho}}_{12} = \xi_{12}\left(|e_{12}| - \psi_{12}\hat{\rho}_{12}\right) \tag{26}$$

where $\xi_{12},\ \psi_{12} \in \mathrm{R}^+$ are the adaptive control parameters, and the estimation error can be defined as $\tilde{\rho}_{12} = \rho_{12} - \hat{\rho}_{12}$.

Step 3: Introduce an error variable again $e_{13} = I_1 - I_{1d}$, and substitute e_{13} into (21) yields

$$\begin{aligned} \dot{V}_{12} = &-k_{11}e_{11}^2 - k_{12}e_{12}^2 + \frac{K_1\bar{R}_1}{\bar{J}_1\eta_1}e_{12}e_{13} + e_{12}\left(\Delta_1 - z_{12}\right. \\ &\left. - \hat{\rho}_{11}\mathrm{sign}\left(e_{12}\right)\right) + e_{12}\left(\lambda_{12} - \dot{V}_{1d} - \hat{\rho}_{12}\mathrm{sign}\left(e_{12}\right)\right) \end{aligned} \tag{27}$$

Next, in order to provide higher control precision and smooth system trajectory, an adaptive method for nonsingular terminal sliding mode (NTSM) control [24] is presented:

$$S_1 = e_{13} + \int_0^t k_{13}\mathrm{sig}^{1+\frac{1}{\alpha_1}}\left(e_{13}\right) + k_{14}\mathrm{sig}^{1-\frac{1}{\alpha_1}}\left(e_{13}\right)d\tau \tag{28}$$

where $\alpha_1 > 1$ is constant, and $k_{13},\ k_{14} \in \mathrm{R}^+$ are the adaptive parameters.

Remark 2: $\mathrm{sig}^{\alpha_i}(x) = |x|^{\alpha_i}\mathrm{sign}(x)$ is used to simplify expression [25].

Traditionally, the parameters $k_{13},\ k_{14}$ for NTSM control method are pre-selected and fixed throughout the entire control process, and this design has improved the control performances of many systems. However, the system's control precision and robust stability can be further improved if the fixed parameters $k_{13},\ k_{14}$ are considered as time-varying parameters. Therefore, an adaptive algorithm is utilized to timely and accurately update the parameters $k_{13},\ k_{14}$ according to the control performance as follows:

$$\dot{k}_{1n} = \begin{cases} -\zeta_{1n} & k_{1n} \ge k_{1n\max} \\ \zeta_{1n}\mathrm{sign}\left(|e_{13}| - \phi_{1n}\right) & k_{1n\min} < k_{1n} < k_{1n\max} \\ \zeta_{1n} & k_{1n} \le k_{1n\min} \end{cases} \tag{29}$$

where $\zeta_{1n},\ \phi_{1n} \in \mathrm{R}^+$; $k_{1n\max}$ and $k_{1n\min}$ stand for the maximum and minimum values of k_{1n}, respectively, $n = 3,\ 4$.

Further, in order to enhance the convergence speed and suppress the chatter phenomena, a fast terminal sliding mode type reaching law [26], [27] is selected as

$$\dot{S}_1 = -g_{11}S_1 - g_{12}\mathrm{sig}^{\vartheta_1}\left(S_1\right) \tag{30}$$

where $g_{11},\ g_{12} \in \mathrm{R}^+$ are the reaching law parameters, and $0 < \vartheta_1 < 1$.

Then combine (28) and (30) together, the ANTSMC for the left coiler tension subsystem sys'$_1$ is designed as

$$\begin{aligned} u_1 = \frac{l_1}{K_{s1}}\Bigg(&\frac{K_1\eta_1}{l_1\bar{R}_1}V_1 + \frac{r_1}{l_1}I_1 + \dot{I}_{1d} - \omega_1 - k_{13}\mathrm{sig}^{1+\frac{1}{\alpha_1}}(e_{13}) \\ &- k_{14}\mathrm{sig}^{1-\frac{1}{\alpha_1}}(e_{13}) - g_{11}S_1 - g_{12}\mathrm{sig}^{\vartheta_1}\left(S_1\right) \\ &- \mathrm{sign}\left(S_1\right)\frac{K_1\bar{R}_1}{\bar{J}_1\eta_1}e_{12}e_{13}\Bigg) \end{aligned} \tag{31}$$

Similarly, another second order sliding mode integral filter is adopted to estimate $\dot{I}_{1d}$ in (31):

$$\begin{cases} \dot{\lambda}_{13} = -\dfrac{\lambda_{13} - I_{1d}}{\tau_{13}} - \dfrac{\gamma_{13}\left(\lambda_{13} - I_{1d}\right)}{\left|\lambda_{13} - I_{1d}\right| + \varepsilon_{13}} \\ \dot{\lambda}_{14} = -\dfrac{\lambda_{14} - \dot{\lambda}_{13}}{\tau_{14}} - \dfrac{\gamma_{14}\left(\lambda_{14} - \dot{\lambda}_{13}\right)}{\left|\lambda_{14} - \dot{\lambda}_{13}\right| + \varepsilon_{14}} \end{cases} \tag{32}$$

where λ_{13} and λ_{14} are the estimation values of I_{1d} and $\dot{I}_{1d}$, respectively. $\tau_{13},\ \tau_{14} \in \mathrm{R}^+$ are the time constants of the filter; $\gamma_{13},\ \gamma_{14},\ \varepsilon_{13},\ \varepsilon_{14} \in \mathrm{R}^+$ are the designed parameters.

Define the estimation error of the adopted second order sliding mode integral filter as $E_{13} = \lambda_{14} - \dot{I}_{1d}$, and we assume E_{13} is bounded, that is, $|E_{13}| \le \rho_{13}$, in which $\rho_{13} \in \mathrm{R}^+$ is the upper bound of E_{13}.

Then (31) can be redesigned as

$$\begin{aligned} u_1 = \frac{l_1}{K_{s1}}\Bigg(&\frac{K_1\eta_1}{l_1\bar{R}_1}V_1 + \frac{r_1}{l_1}I_1 + \lambda_{14} - \omega_1 - k_{13}\mathrm{sig}^{1+\frac{1}{\alpha_1}}(e_{13}) \\ &- k_{14}\mathrm{sig}^{1-\frac{1}{\alpha_1}}(e_{13}) - g_{11}S_1 - g_{12}\mathrm{sig}^{\vartheta_2}(S_1) \\ &- \hat{\rho}_{13}\mathrm{sign}(S_1) - \mathrm{sign}(S_1)\frac{K_1\bar{R}_1}{\bar{J}_1\eta_1}e_{12}e_{13}\Bigg) \end{aligned} \tag{33}$$

where $\hat{\rho}_{13}$ is the estimation value of ρ_{13}, and the adaptive law can be designed as

$$\dot{\hat{\rho}}_{13} = \xi_{13}\left(|\mathrm{sign}\left(S_1\right)| - \psi_{13}\hat{\rho}_{13}\right) \tag{34}$$

where $\xi_{13},\ \psi_{13} \in \mathrm{R}^+$ are the adaptive control parameters, and the estimation error can be defined as $\tilde{\rho}_{13} = \rho_{13} - \hat{\rho}_{13}$.

Secondly, we focus on the main rolling mill speed subsystem sys'$_2$.

Step 1: By (2b), the tracking error of the main rolling mill speed is defined as $e_{21} = V_2 - V_2^*$, and the time derivative of e_{21} is

$$\dot{e}_{21} = \frac{K_2R_2}{J_2\eta_2}I_2 + \frac{R_2^2}{J_2\eta_2^2}(F_3 - F_1) - \frac{B_{u2}}{J_2}V_2 - \frac{M_zR_2}{J_2\eta_2^2} + \Delta_2 - \dot{V}_2^* \quad (35)$$

where V_2^* is the given value of the main rolling mill speed subsystem.

Choose the Lyapunov function candidate as $V_{21} = \frac{1}{2}e_{21}^2$, and the time derivative of V_{21} is

$$\dot{V}_{21} = e_{21}\left(\frac{K_2R_2}{J_2\eta_2}I_2 + \frac{R_2^2}{J_2\eta_2^2}(F_3 - F_1) - \frac{B_{u2}}{J_2}V_2 - \frac{M_zR_2}{J_2\eta_2^2} + \Delta_2 - \dot{V}_2^*\right) \quad (36)$$

By (36), the virtual control variable I_{2d} can be designed as

$$I_{2d} = \frac{J_2\eta_2}{K_2R_2}\left(-\frac{R_2^2}{J_2\eta_2^2}(F_3 - F_1) + \frac{B_{u2}}{J_2}V_2 - z_{22} + \dot{V}_2^* - k_{21}e_{21} - \hat{\rho}_{21}\text{sign}(e_{21}) + \frac{M_ZR_2}{J_2\eta_2^2}\right) \quad (37)$$

where $k_{21} \in \mathrm{R}^+$ is the control parameter; $\hat{\rho}_{21}$ is the estimation value of ρ_{21}, and the adaptive law can be designed as

$$\dot{\hat{\rho}}_{21} = \xi_{21}\left(|e_{21}| - \psi_{21}\hat{\rho}_{21}\right) \quad (38)$$

where ξ_{21}, $\psi_{21} \in \mathrm{R}^+$ are the adaptive control parameters, and the estimation error can be defined as $\tilde{\rho}_{21} = \rho_{21} - \hat{\rho}_{21}$.

Step 2: Introduce an error variable $e_{22} = I_2 - I_{2d}$, and substitute e_{22} into (36) yields

$$\dot{V}_{21} = -k_{21}e_{21}^2 + \frac{K_2R_2}{J_2\eta_2}e_{21}e_{22} + e_{21}(\Delta_2 - z_{22} - \hat{\rho}_{21}\text{sign}(e_{21})) \quad (39)$$

Similarly, the ANTSM surface [24] S_2 is defined as

$$S_2 = e_{22} + \int_0^t k_{22}\text{sig}^{1+\frac{1}{\alpha_2}}(e_{22}) + k_{23}\text{sig}^{1-\frac{1}{\alpha_2}}(e_{22})\,d\tau \quad (40)$$

where $\alpha_2 > 1$ is constant, k_{22}, $k_{23} \in \mathrm{R}^+$ are the adaptive parameters, and their design forms are as follows:

$$\dot{k}_{2j} = \begin{cases} -\zeta_{2j} & k_{2j} \geq k_{2j\max} \\ \zeta_{2j}\text{sign}\left(|e_{22}| - \phi_{2j}\right) & k_{2j\min} < k_{2j} < k_{2j\max} \\ \zeta_{2j} & k_{2j} \leq k_{2j\min} \end{cases} \quad (41)$$

where ζ_{2j}, $\phi_{2j} \in \mathrm{R}^+$; and $k_{2j\max}$, $k_{2j\min}$ stand for the maximum and minimum values of k_{2j}, respectively, $j = 2, 3$.

Further, a fast terminal sliding mode type reaching law is selected as

$$\dot{S}_2 = -g_{21}S_2 - g_{22}\text{sig}^{\vartheta_2}(S_2) \quad (42)$$

where g_{11}, $g_{12} \in \mathrm{R}^+$ are the reaching law parameters, and $0 < \vartheta_2 < 1$.

Then combine (40) and (42) together, the ANTSMC for the main rolling mill speed subsystem sys'$_2$ is designed as

$$u_2 = \frac{l_2}{K_{s2}}\left(\frac{K_2\eta_2}{l_2R_2}V_2 + \frac{r_2}{l_2}I_2 + \dot{I}_{2d} - \omega_2 - k_{22}\text{sig}^{1+\frac{1}{\alpha_2}}(e_{22}) - k_{23}\text{sig}^{1-\frac{1}{\alpha_2}}(e_{22}) - g_{21}S_2 - g_{22}\text{sig}^{\vartheta_2}(S_2) - \text{sign}(S_2)\frac{K_2R_2}{J_2\eta_2}e_{21}e_{22}\right) \quad (43)$$

Considering $\dot{I}_{2d}$ in (43) is difficult to be calculated directly, thus a second order sliding mode integral filter is adopted to estimate $\dot{I}_{2d}$:

$$\begin{cases} \dot{\lambda}_{21} = -\dfrac{\lambda_{21} - I_{2d}}{\tau_{21}} - \dfrac{\gamma_{21}(\lambda_{21} - I_{2d})}{|\lambda_{21} - I_{2d}| + \varepsilon_{21}} \\ \dot{\lambda}_{22} = -\dfrac{\lambda_{22} - \dot{\lambda}_{21}}{\tau_{22}} - \dfrac{\gamma_{22}\left(\lambda_{22} - \dot{\lambda}_{21}\right)}{\left|\lambda_{22} - \dot{\lambda}_{21}\right| + \varepsilon_{22}} \end{cases} \quad (44)$$

where λ_{21} and λ_{22} are the estimation values of V_{2d} and $\dot{V}_{2d}$, respectively. τ_{21}, $\tau_{22} \in \mathrm{R}^+$ are the time constants of the filter; γ_{21}, γ_{22}, ε_{21}, $\varepsilon_{22} \in \mathrm{R}^+$ are the designed parameters.

Define the estimation error of the adopted second order sliding mode integral filter as $E_{22} = \lambda_{22} - \dot{I}_{2d}$, and we assume E_{13} is bounded, that is, $|E_{22}| \leq \rho_{22}$, in which $\rho_{22} \in \mathrm{R}^+$ is the upper bound of E_{22}.

Then (43) can be redesigned as

$$u_2 = \frac{l_2}{K_{s2}}\left(\frac{K_2\eta_2}{l_2R_2}V_2 + \frac{r_2}{l_2}I_2 + \lambda_{22} - \omega_2 - \hat{\rho}_{22}\text{sign}(S_2) - k_{22}\text{sig}^{1+\frac{1}{\alpha_2}}(e_{22}) - k_{23}\text{sig}^{1-\frac{1}{\alpha_2}}(e_{22}) - g_{21}S_2 - g_{22}\text{sig}^{\vartheta_2}(S_2) - \text{sign}(S_2)\frac{K_2R_2}{J_2\eta_2}e_{21}e_{22}\right) \quad (45)$$

where $\hat{\rho}_{22}$ is the estimation value of ρ_{22}, and the adaptive law can be designed as

$$\dot{\hat{\rho}}_{22} = \xi_{22}\left(|\text{sign}(S_2)| - \psi_{22}\hat{\rho}_{22}\right) \quad (46)$$

where ξ_{22}, $\psi_{22} \in \mathrm{R}^+$ are the adaptive control parameters; and the estimation error can be defined as $\tilde{\rho}_{22} = \rho_{22} - \hat{\rho}_{22}$.

Finally, considering the analysis process of the right coiler tension subsystem sys'$_3$ is similar with the left coiler tension subsystem sys'$_1$, then the virtual control variables, the second order sliding mode integral filters, the ANTSM surface [24] S_3, the fast terminal sliding mode type reaching law, and the ANTSMC u_3 can be respectively designed as

$$V_{3d} = V_2(1 + \delta_0(1 + K_\delta F_3)) + \frac{L}{EA_2}\dot{F}_3^* - \frac{L}{EA_2}k_{31}e_{31} \quad (47)$$

$$I_{3d} = \frac{\bar{J}_3\eta_3}{K_3\bar{R}_3}\left(\frac{\bar{R}_3^2}{\bar{J}_3\eta_3^2}F_3 + \frac{B_{u3}}{\bar{J}_3}V_3 - z_{32} + \lambda_{32} - \frac{EA_2}{L}e_{31} - k_{32}e_{32} - \hat{\rho}_{31}\text{sign}(e_{32}) - \hat{\rho}_{32}\text{sign}(e_{32})\right) \quad (48)$$

$$\begin{cases} \dot{\lambda}_{31} = -\dfrac{\lambda_{31} - V_{3d}}{\tau_{31}} - \dfrac{\gamma_{31}(\lambda_{31} - V_{3d})}{|\lambda_{31} - V_{3d}| + \varepsilon_{31}} \\ \dot{\lambda}_{32} = -\dfrac{\lambda_{32} - \dot{\lambda}_{31}}{\tau_{32}} - \dfrac{\gamma_{32}\left(\lambda_{32} - \dot{\lambda}_{31}\right)}{\left|\lambda_{32} - \dot{\lambda}_{31}\right| + \varepsilon_{32}} \end{cases} \quad (49)$$

$$\begin{cases} \dot{\lambda}_{33} = -\dfrac{\lambda_{33} - I_{3d}}{\tau_{33}} - \dfrac{\gamma_{33}\left(\lambda_{33} - I_{3d}\right)}{\left|\lambda_{33} - I_{3d}\right| + \varepsilon_{33}} \\ \dot{\lambda}_{34} = -\dfrac{\lambda_{34} - \dot{\lambda}_{33}}{\tau_{34}} - \dfrac{\gamma_{34}\left(\lambda_{34} - \dot{\lambda}_{33}\right)}{\left|\lambda_{34} - \dot{\lambda}_{33}\right| + \varepsilon_{34}} \end{cases} \tag{50}$$

$$S_3 = e_{33} + \int_0^t k_{33}\mathrm{sig}^{1+\frac{1}{\alpha_3}}(e_{33}) + k_{34}\mathrm{sig}^{1-\frac{1}{\alpha_3}}(e_{33})\,d\tau \tag{51}$$

$$\dot{S}_3 = -g_{31}S_3 - g_{32}\mathrm{sig}^{\vartheta_3}(S_3) \tag{52}$$

$$\begin{aligned} u_3 = \frac{l_3}{K_{s3}}\Bigg(&\frac{K_3\eta_3}{l_3\bar{R}_3}V_3 + \frac{r_3}{l_3}I_3 + \lambda_{34} - \omega_3 - k_{33}\mathrm{sig}^{1+\frac{1}{\alpha_3}}(e_{33}) \\ &- k_{34}\mathrm{sig}^{1-\frac{1}{\alpha_3}}(e_{33}) - g_{31}S_3 - g_{32}\mathrm{sig}^{\vartheta_3}(S_3) \\ &- \hat{\rho}_{33}\mathrm{sign}(S_3) - \mathrm{sign}(S_3)\frac{K_3\bar{R}_3}{\bar{J}_3\eta_3}e_{32}e_{33}\Bigg) \end{aligned} \tag{53}$$

$$\begin{cases} \dot{\hat{\rho}}_{31} = \xi_{31}\left(|e_{32}| - \psi_{31}\hat{\rho}_{31}\right) \\ \dot{\hat{\rho}}_{32} = \xi_{32}\left(|e_{32}| - \psi_{32}\hat{\rho}_{32}\right) \\ \dot{\hat{\rho}}_{33} = \xi_{33}\left(|\mathrm{sign}(S_3)| - \psi_{33}\hat{\rho}_{33}\right) \end{cases} \tag{54}$$

where F_3^* is the given value of the right coiler tension subsystem sys'$_3$; $e_{31} = F_3 - F_3^*$, $e_{32} = V_3 - V_{3d}$ and $e_{33} = I_3 - I_{3d}$ are the error variables; ξ_{31}, ξ_{32}, ξ_{33}, ψ_{31}, ψ_{32}, $\psi_{33} \in \mathrm{R}^+$ are the adaptive control parameters, and the estimation errors can be defined as $\tilde{\rho}_{31} = \rho_{31} - \hat{\rho}_{31}$, $\tilde{\rho}_{32} = \rho_{32} - \hat{\rho}_{32}$ and $\tilde{\rho}_{33} = \rho_{33} - \hat{\rho}_{33}$; λ_{31}, λ_{32}, λ_{33} and λ_{34} are the estimation values of V_{3d}, $\dot{V}_{3d}$, I_{3d} and $\dot{I}_{3d}$, respectively; g_{31}, $g_{32} \in \mathrm{R}^+$ are the reaching law parameters, and $0 < \vartheta_3 < 1$; k_{31}, $k_{32} \in \mathrm{R}^+$ are the control parameters, τ_{31}, τ_{32}, τ_{33}, $\tau_{34} \in \mathrm{R}^+$ are the time constants of the filters, γ_{31}, γ_{32}, γ_{33}, γ_{34}, ε_{31}, ε_{32}, ε_{33}, $\varepsilon_{34} \in \mathrm{R}^+$ are the designed parameters; k_{33}, $k_{34} \in \mathrm{R}^+$ are the adaptive parameters, and their design forms are as follows:

$$\dot{k}_{3f} = \begin{cases} -\zeta_{3f} & k_{3f} \geq k_{3f\,\max} \\ \zeta_{3f}\mathrm{sign}\left(|e_{33}| - \phi_{3f}\right) & k_{3f\,\min} < k_{3f} < k_{3f\,\max} \\ \zeta_{3f} & k_{3f} \leq k_{3f\,\min} \end{cases} \tag{55}$$

where ζ_{3f}, $\phi_{3f} \in \mathrm{R}^+$; $k_{3f\,\max}$ and $k_{3f\,\min}$ stand for the maximum and minimum values of k_{3f}, respectively, $f = 3,\ 4$.

Remark 3: Through the analysis of the adaptive algorithms (29), (41), and (55), it can be seen that when the control precision does not satisfy $|e| - \phi \leq 0$, then the adaptive parameter k will increase, and the larger parameter k can effectively suppress the control error, so as to obtain higher control precision. On the other hand, when the control precision satisfies $|e| - \phi \leq 0$, k will decrease to obtain relatively smooth system trajectory.

In the designed controllers (33), (45), and (53), the matched uncertainty ω_i is complex and unknown. Considering the neural network adaptive method can effectively approximate any continuous function online, thus it will be adopted to approximate ω_i in the next step.

B. NEURAL NETWORK ADAPTIVE APPROXIMATIONS FOR THE MATCHED UNCERTAINTIES

According to the following approximation theorem of neural network [19]:

$$\omega = \boldsymbol{W}^T\boldsymbol{h}(\boldsymbol{x}) + \sigma \tag{56}$$

where $\boldsymbol{W} = (W_1, W_2, \cdots, W_m)^T$ is the ideal network weight vector, and consider it is difficult to obtain directly, then $\hat{\boldsymbol{W}}$ can be used to conduct adaptive estimation for $\boldsymbol{W}$; $\boldsymbol{h}(\boldsymbol{x}) = (h_1(\boldsymbol{x}), h_2(\boldsymbol{x}), \cdots, h_m(\boldsymbol{x}))^T$ is the basis function vector, and the yth item $h_y(\boldsymbol{x}) = \exp\left(-\frac{(\boldsymbol{x}-\boldsymbol{\iota}_y)^2}{2\varpi_y^2}\right)$, $y = 1, \cdots, m$, in which $\boldsymbol{\iota}_y \in \mathrm{R}^N$ is the center point of $h_y(\boldsymbol{x})$, $\varpi_y \in \mathrm{R}^+$ is the base width of $h_y(\boldsymbol{x})$; $\boldsymbol{x} \in \mathrm{R}^+$ is the input vector; σ is the approximation error of neural network.

Then for the matched uncertainty ω_i in (33), (45), and (53), the input vectors of the adopted RBF neural networks are chosen as $\boldsymbol{x}_1 = [e_{11}\ e_{12}\ e_{13}]$, $\boldsymbol{x}_2 = [e_{21}\ e_{22}]$, $\boldsymbol{x}_3 = [e_{31}\ e_{32}\ e_{33}]$, and the approximation error σ_i satisfies $|\sigma_1| \leq \rho_{14}$, $|\sigma_2| \leq \rho_{23}$, and $|\sigma_3| \leq \rho_{34}$, in which ρ_{14}, ρ_{23}, and ρ_{34} are the unknown upper bounds of σ_1, σ_2, and σ_3, respectively. Then based on (33), (45), (53), and (56), the ANTSMCs for the speed and tension system of the reversible cold strip rolling mill can be finally designed as

$$\begin{aligned} u_1 = \frac{l_1}{K_{s1}}\Bigg(&\frac{K_1\eta_1}{l_1\bar{R}_1}V_1 + \frac{r_1}{l_1}I_1 + \lambda_{14} - \hat{\boldsymbol{W}}_1^{\mathrm{T}}\boldsymbol{h}(\boldsymbol{x}) - g_{11}S_1 \\ &- k_{13}\mathrm{sig}^{1+\frac{1}{\alpha_1}}(e_{13}) - k_{14}\mathrm{sig}^{1-\frac{1}{\alpha_1}}(e_{13}) - g_{12}\mathrm{sig}^{\vartheta_1}(S_1) \\ &- \hat{\rho}_{13}\mathrm{sign}(S_1) - \hat{\rho}_{14}\mathrm{sign}(S_1) - \mathrm{sign}(S_1)\frac{K_1\bar{R}_1}{\bar{J}_1\eta_1}e_{12}e_{13}\Bigg) \end{aligned} \tag{57}$$

$$\begin{aligned} u_2 = \frac{l_2}{K_{s2}}\Bigg(&\frac{K_2\eta_2}{l_2R_2}V_2 + \frac{r_2}{l_2}I_2 + \lambda_{22} - \hat{\boldsymbol{W}}_2^{\mathrm{T}}\boldsymbol{h}(\boldsymbol{x}) \\ &- k_{22}\mathrm{sig}^{1+\frac{1}{\alpha_2}}(e_{22}) - k_{23}\mathrm{sig}^{1-\frac{1}{\alpha_2}}(e_{22}) \\ &- g_{21}S_2 - g_{22}\mathrm{sig}^{\vartheta_2}(S_2) - \hat{\rho}_{22}\mathrm{sign}(S_2) \\ &- \hat{\rho}_{23}\mathrm{sign}(S_2) - \mathrm{sign}(S_2)\frac{K_2R_2}{J_2\eta_2}e_{21}e_{22}\Bigg) \end{aligned} \tag{58}$$

$$\begin{aligned} u_3 = \frac{l_3}{K_{s3}}\Bigg(&\frac{K_3\eta_3}{l_3\bar{R}_3}V_3 + \frac{r_3}{l_3}I_3 + \lambda_{34} - \hat{\boldsymbol{W}}_3^{\mathrm{T}}\boldsymbol{h}(\boldsymbol{x}) \\ &- k_{33}\mathrm{sig}^{1+\frac{1}{\alpha_3}}(e_{33}) - k_{34}\mathrm{sig}^{1-\frac{1}{\alpha_3}}(e_{33}) \\ &- g_{31}S_3 - g_{32}\mathrm{sig}^{\vartheta_3}(S_3) - \hat{\rho}_{33}\mathrm{sign}(S_3) \\ &- \hat{\rho}_{34}\mathrm{sign}(S_3) - \mathrm{sign}(S_3)\frac{K_3\bar{R}_3}{\bar{J}_3\eta_3}e_{32}e_{33}\Bigg) \end{aligned} \tag{59}$$

And the adaptive laws can be designed as

$$\begin{cases} \dot{\hat{\boldsymbol{W}}}_1 = d_1\left(\mathrm{sign}(S_1)\,\boldsymbol{h}(\boldsymbol{x}) - b_1\hat{\boldsymbol{W}}_1\right) \\ \dot{\hat{\rho}}_{14} = \xi_{14}\left(|\mathrm{sign}(S_1)| - \psi_{14}\hat{\rho}_{14}\right) \\ \dot{\hat{\boldsymbol{W}}}_2 = d_2\left(\mathrm{sign}(S_2)\,\boldsymbol{h}(\boldsymbol{x}) - b_2\hat{\boldsymbol{W}}_2\right) \\ \dot{\hat{\rho}}_{23} = \xi_{23}\left(|\mathrm{sign}(S_2)| - \psi_{23}\hat{\rho}_{23}\right) \\ \dot{\hat{\boldsymbol{W}}}_3 = d_3\left(\mathrm{sign}(S_3)\,\boldsymbol{h}(\boldsymbol{x}) - b_3\hat{\boldsymbol{W}}_3\right) \\ \dot{\hat{\rho}}_{34} = \xi_{34}\left(|\mathrm{sign}(S_3)| - \psi_{34}\hat{\rho}_{34}\right) \end{cases} \tag{60}$$

where d_i, b_i, ξ_{14}, ψ_{14}, ξ_{23}, ψ_{23}, ξ_{34}, $\psi_{34} \in \mathrm{R}^+$ are the adaptive control parameters, and the estimation errors can be defined as $\tilde{\rho}_{14} = \rho_{14} - \hat{\rho}_{14}$, $\tilde{\rho}_{23} = \rho_{23} - \hat{\rho}_{23}$, $\tilde{\rho}_{34} = \rho_{34} - \hat{\rho}_{34}$, and $\tilde{\boldsymbol{W}}_i = \boldsymbol{W}_i - \hat{\boldsymbol{W}}_i$.

V. ANALYSES OF STABILITY AND CONVERGENCE FOR THE SPEED AND TENSION SYSTEM

A. STABILITY ANALYSIS

Theorem 2: For the speed and tension system (2) of the reversible cold strip rolling mill, if we adopt the second order sliding mode integral filters (24), (32), (44), (49), and (50), choose the ANTSM surfaces (28), (40), and (51), design the ANTSMCs (57), (58), and (59), then the speed and tension system (2) of the reversible cold strip rolling mill is stable.

Proof: For simplicity, take the main rolling mill speed subsystem sys'$_2$ as an example for the stability analysis, and the Lyapunov function candidate is chosen as

$$V_{22} = V_{21} + |S_2| + \frac{\tilde{\rho}_{21}^2}{2\xi_{21}} + \frac{\tilde{\rho}_{22}^2}{2\xi_{22}} + \frac{\tilde{\rho}_{23}^2}{2\xi_{23}} + \frac{\tilde{\boldsymbol{W}}_2^T \tilde{\boldsymbol{W}}_2}{2d_2} \tag{61}$$

Substitute (38), (39), (40), (42), (46), (58), and (60) into the time derivative of (61), and there is

$$\begin{aligned}
&\dot{V}_{22} \\
&= \dot{V}_{21} + \dot{S}_2 \mathrm{sign}(S_2) - \sum_{i=1}^{3} \frac{\tilde{\rho}_{2i}\dot{\tilde{\rho}}_{2i}}{\xi_{2i}} - \frac{\tilde{\boldsymbol{W}}_2^T \dot{\tilde{\boldsymbol{W}}}_2}{d_2} \\
&= -k_{21}e_{21}^2 + e_{21}\left(\Delta_2 - z_{22} - \hat{\rho}_{21}\mathrm{sign}\left(e_{21}\right)\right) + \frac{K_2 R_2}{J_2 \eta_2} e_{21} e_{22} \\
&\quad + \mathrm{sign}\left(S_2\right)\left(\lambda_{22} - \dot{I}_{2d} - \hat{\rho}_{22}\mathrm{sign}\left(S_2\right) - g_{21}S_2\right. \\
&\quad \left. - g_{22}\mathrm{sig}^{\vartheta_2}\left(S_2\right) - \mathrm{sign}\left(S_2\right)\frac{K_2 R_2}{J_2 \eta_2} e_{21} e_{22} + \omega_2 - \hat{\boldsymbol{W}}_2^T \boldsymbol{h}(\boldsymbol{x})\right. \\
&\quad \left. - \hat{\rho}_{23}\mathrm{sign}\left(S_2\right)\right) - \frac{\tilde{\rho}_{21}\dot{\tilde{\rho}}_{21}}{\xi_{21}} - \frac{\tilde{\rho}_{22}\dot{\tilde{\rho}}_{22}}{\xi_{22}} - \frac{\tilde{\rho}_{23}\dot{\tilde{\rho}}_{23}}{\xi_{23}} - \frac{\tilde{\boldsymbol{W}}_2^T \dot{\tilde{\boldsymbol{W}}}_2}{d_2} \\
&\leq -k_{21}e_{21}^2 - g_{21}\left|S_2\right| - g_{22}\left|S_2\right|^{\vartheta_2} + e_{21}\left(\rho_{21} - \hat{\rho}_{21}\mathrm{sign}\left(e_{21}\right)\right) \\
&\quad + \mathrm{sign}\left(S_2\right)\left(\tilde{\boldsymbol{W}}_2^T \boldsymbol{h}(\boldsymbol{x}) + \rho_{23} - \hat{\rho}_{23}\mathrm{sign}\left(S_2\right)\right) - \frac{\tilde{\rho}_{21}\dot{\tilde{\rho}}_{21}}{\xi_{21}} \\
&\quad + \mathrm{sign}\left(S_2\right)\left(\rho_{22} - \hat{\rho}_{22}\mathrm{sign}\left(S_2\right)\right) - \frac{\tilde{\rho}_{22}\dot{\tilde{\rho}}_{22}}{\xi_{22}} - \frac{\tilde{\rho}_{23}\dot{\tilde{\rho}}_{23}}{\xi_{23}} \\
&\quad - \frac{\tilde{\boldsymbol{W}}_2^T \dot{\tilde{\boldsymbol{W}}}_2}{d_2}
\end{aligned} \tag{62}$$

According to $-2ab \leq a^2 + b^2$, then (62) can be rewritten as

$$\begin{aligned}
\dot{V}_{22} &\leq -k_{21}e_{21}^2 - g_{21}\left|S_2\right| - \frac{\psi_{21}}{2}\tilde{\rho}_{21}^2 - \frac{\psi_{22}}{2}\tilde{\rho}_{22}^2 \\
&\quad - \frac{\psi_{23}}{2}\tilde{\rho}_{23}^2 - \frac{b_2}{2}\tilde{\boldsymbol{W}}_2^T \tilde{\boldsymbol{W}}_2 + \frac{\psi_{21}}{2}\rho_{21}^2 \\
&\quad + \frac{\psi_{22}}{2}\rho_{22}^2 + \frac{\psi_{23}}{2}\rho_{23}^2 + \frac{b_2}{2}\boldsymbol{W}_2^T \boldsymbol{W}_2 \\
&\leq -k_{21}e_{21}^2 - C_2\left|S_2\right| - \frac{\psi_{21}}{2}\tilde{\rho}_{21}^2 - \frac{\psi_{22}}{2}\tilde{\rho}_{22}^2 \\
&\quad - \frac{\psi_{23}}{2}\tilde{\rho}_{23}^2 - \frac{b_2}{2}\tilde{\boldsymbol{W}}_2^T \tilde{\boldsymbol{W}}_2
\end{aligned} \tag{63}$$

where $C_1 = \frac{\psi_{21}}{2}\rho_{21}^2 + \frac{\psi_{22}}{2}\rho_{22}^2 + \frac{\psi_{23}}{2}\rho_{23}^2 + \frac{b_2}{2}\boldsymbol{W}_2^T \boldsymbol{W}_2$, and $C_2 = g_{21} - C_1\left|S_2\right|^{-1}$.

Under the condition that $C_2 > 0$, i.e. $|S_2| > \frac{C_1}{g_{21}}$, and there is

$$\dot{V}_{22} < -\delta_2 V_{22} < 0 \tag{64}$$

where $\delta_2 = \min\left\{2k_{21}, C_2, \psi_{21}\xi_{21}, \psi_{22}\xi_{22}, \psi_{23}\xi_{23}, b_2 d_2\right\}$.

By (64), we can get the subsystem sys'$_2$ is stable, and the following bound can be reached

$$|S_2| \leq C_3 \tag{65}$$

where $C_3 = C_1/g_{21}$.

Equation (65) implies that the ANTSM variable S_2 can converge to $|S_2| \leq C_3$, and the main rolling mill speed subsystem sys'$_2$ can converge to any arbitrary neighbourhood of the sliding surface S_2 by selecting appropriate parameters.

Next, substitute (42) into the time derivative of (40), and we have

$$\begin{aligned}
&\dot{e}_{22} + k_{22}\mathrm{sig}^{1+\frac{1}{\alpha_2}}\left(e_{22}\right) + k_{23}\mathrm{sig}^{1-\frac{1}{\alpha_2}}\left(e_{22}\right) \\
&\qquad = -g_{21}S_2 - g_{22}\mathrm{sig}^{\vartheta_2}\left(S_2\right)
\end{aligned} \tag{66}$$

The analysis process in [28] can be applied to (66), and then (66) can be rearranged as the following two forms:

$$\dot{e}_{22} + \widehat{k}_{22}\mathrm{sig}^{1+\frac{1}{\alpha_2}}\left(e_{22}\right) + k_{23}\mathrm{sig}^{1-\frac{1}{\alpha_2}}\left(e_{22}\right) = 0 \tag{67}$$

and

$$\dot{e}_{22} + k_{22}\mathrm{sig}^{1+\frac{1}{\alpha_2}}\left(e_{22}\right) + \widehat{k}_{23}\mathrm{sig}^{1-\frac{1}{\alpha_2}}\left(e_{22}\right) = 0 \tag{68}$$

where $\widehat{k}_{22} = k_{22} + \left(g_{21}S_2 + g_{22}\mathrm{sig}^{\vartheta_2}\left(S_2\right)\right)\mathrm{sig}^{-\left(1+\frac{1}{\alpha_2}\right)}\left(e_{22}\right)$, $\widehat{k}_{23} = k_{23} + \left(g_{21}S_2 + g_{22}\mathrm{sig}^{\vartheta_2}\left(S_2\right)\right)\mathrm{sig}^{-\left(1-\frac{1}{\alpha_2}\right)}\left(e_{22}\right)$.

If $\widehat{k}_{22} > 0$, the error dynamics (67) can be regarded as $\dot{S}_2$ (the derivative form of ANTSM S_2). Considering $|S_2| \leq C_3$, then one can show the convergence of the error variable e_{22} from the following condition:

$$\widehat{k}_{22\min} = k_{22\min} - \left(g_{21}\left|C_3\right| + g_{22}\left|C_3\right|^{\vartheta_2}\right)\left|e_{22}\right|^{-\left(1+\frac{1}{\alpha_2}\right)} > 0 \tag{69}$$

By (69), the error variable e_{22} can converge to

$$|e_{22}| \leq q_1 \tag{70}$$

where $q_1 = \left(\frac{g_{21}|C_3| + g_{22}|C_3|^{\vartheta_2}}{k_{22\min}}\right)^{\frac{1}{1+\frac{1}{\alpha_2}}}$.

Similarly, if $\widehat{k}_{23} > 0$, the error dynamics (68) can be regarded as $\dot{S}_2$, then the error variable e_{22} can converge to

$$|e_{22}| \leq q_2 \tag{71}$$

where $q_2 = \left(\frac{g_{21}|C_3| + g_{22}|C_3|^{\vartheta_2}}{k_{23\min}}\right)^{\frac{1}{1-\frac{1}{\alpha_2}}}$.

Combine (70) and (71) together, and the error variable e_{22} can converge to

$$|e_{22}| \leq q_{\min} \tag{72}$$

where $q_{\min} = \min\left\{q_1, q_2\right\}$.

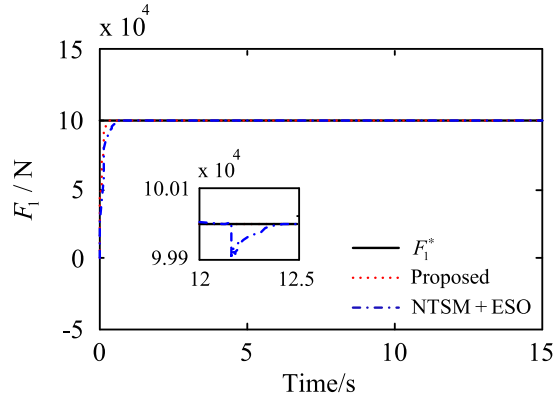

(a) Tension tracking control response curves of the left coiler

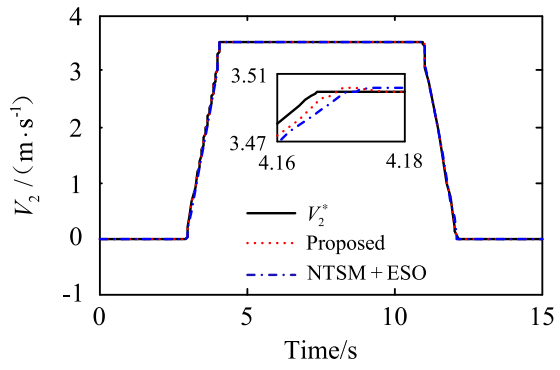

(b) Speed tracking control response curves of the main rolling mill

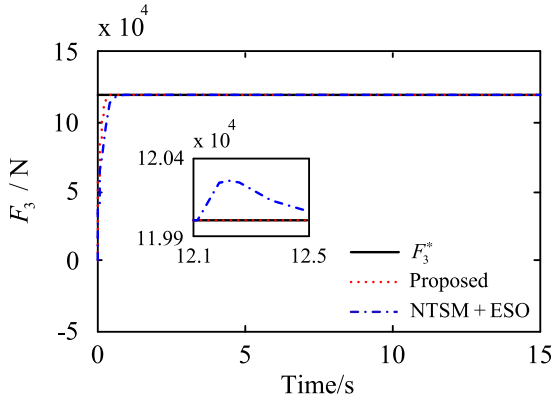

(c) Tension tracking control response curves of the right coiler

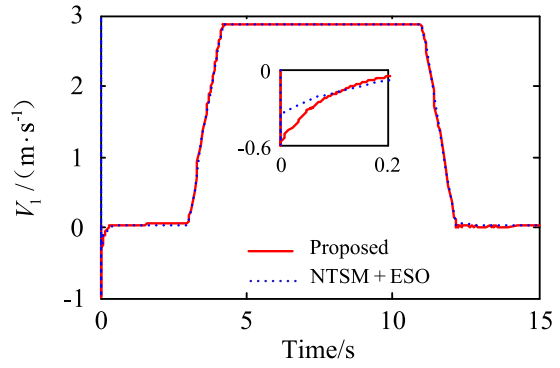

(d) Speed response curves of the left coiler

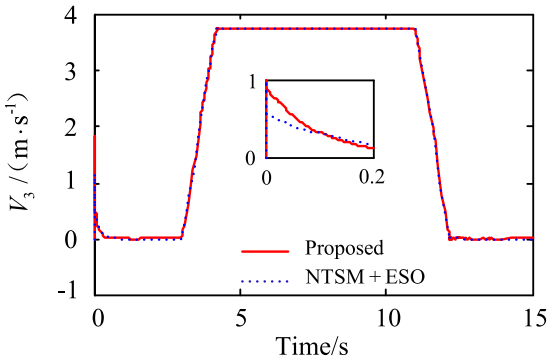

(e) Speed response curves of the right coiler

FIGURE 2. Coordinated tracking control response curves of the reversible cold strip rolling mill.

Up to this point, it can be concluded that the main rolling mill speed subsystem sys'$_2$ is stable, and the system trajectories S_2 and e_{22} can converge to the bounds (65) and (72), respectively.

B. CONVERGENCE ANALYSIS

Theorem 3: For the speed and tension system (2) of the reversible cold strip rolling mill, if we choose the ANTSM surfaces (28), (40), and (51), the fast terminal sliding mode type reaching laws (30), (42), and (52), then the ANTSM variables can converge to bounds in finite time.

Proof: For simplicity, we also take the main rolling mill speed subsystem sys'$_2$ as an example for the convergence analysis.

Suppose the initial state of sliding mode variable S_2 satisfies $S_2(0) > C_3$, and according to (42), the convergence time

of S_2 from initial state $S_2(0)$ to $S_2 = C_3$ is determined by

$$\begin{aligned} T_2 &= \int_{S_2(0)}^{C_3} \frac{\mathrm{d}S_2}{-g_{21}S_2 - g_{22}S_2^{\vartheta_2}} \\ &= \int_{C_3}^{S_2(0)} \frac{\mathrm{d}S_2}{g_{21}S_2 + g_{22}S_2^{\vartheta_2}} \\ &= \int_{C_3}^{S_2(0)} \frac{S_2^{-\vartheta_2}\mathrm{d}S_2}{g_{21}S_2^{1-\vartheta_2} + g_{22}} \\ &= \frac{1}{1-\vartheta_2} \int_{C_3}^{S_2(0)} \frac{\mathrm{d}S_2^{1-\vartheta_2}}{g_{21}S_2^{1-\vartheta_2} + g_{22}} \end{aligned} \tag{73}$$

Based on (73), and choose an alternate variable $z_2 = S_2^{1-\vartheta_2}$, then the following can be obtained:

$$T_2 = \frac{1}{1-\vartheta_2} \int_{C_3^{1-\vartheta_2}}^{S_2(0)^{1-\vartheta_2}} \frac{\mathrm{d}z_2}{g_{21}z_2 + g_{22}} \tag{74}$$

Make $g_{21}z_2 + g_{22} > 0$ by selecting parameters g_{21} and g_{22}, and we can further get

$$\begin{aligned} T_2 &= \frac{1}{g_{21}(1-\vartheta_2)} \ln(g_{21}z_2 + g_{22}) \Big|_{C_3^{1-\vartheta_2}}^{S_2(0)^{1-\vartheta_2}} \\ &= \frac{1}{g_{21}(1-\vartheta_2)} \ln\left(\frac{g_{21}S_2(0)^{1-\vartheta_2} + g_{22}}{g_{21}C_3^{1-\vartheta_2} + g_{22}}\right) \end{aligned} \tag{75}$$

By (75), it can be concluded that the ANTSM variable S_2 can converge to the bound (65) in finite time T_2.

Remark 4: If the initial state of sliding mode variable S_2 satisfies $S_2(0) < -C_3$, we can get similar result.

Remark 5: Owing to the analyses of stability and convergence for the left coiler tension subsystem sys'$_1$ and the right coiler tension subsystem sys'$_3$ are similar with the main rolling mill speed subsystem sys'$_2$, the processes in this section will not be repeated.

VI. SIMULATION RESEARCH

In this section, the simulation research is carried out on the speed and tension system of a 1422 mm reversible cold strip rolling mill by using actual data, and through comparing with the traditional NTSM backstepping control strategy based on ESO to verify the validity of the proposed control strategy.

Choose the actual rolling parameters of a rolling schedule as follows: $R_1 = 0.89$ m, $R_2 = 0.20635$ m, $R_3 = 0.255$ m, $\bar{R}_1 = 0.5$ m, $\bar{R}_3 = 0.45$ m; $J_1 = 3347$ kg $\cdot$ m^2, $J_2 = 1274.5$kg $\cdot$ m^2, $J_3 = 406.7$ kg $\cdot$ m^2, $\bar{J}_1 = \bar{J}_3 = 1800$ kg $\cdot$ m^2; $\delta_0 = 0.065$, $\chi_0 = 0.182$, $K_\delta = 5 \times 10^{-8}$, $K_\chi = 6.511 \times 10^{-8}$; $M_z = 25$ kN $\cdot$ m; $E = 2.508 \times 10^9$ N/m^2; $H = 2.06 \times 10^{-3}$ m, $h = 1.582 \times 10^{-3}$ m; $L = 3$ m; $B_{u1} = B_{u3} = 0.3014$ kg $\cdot$ m^2/s, $B_{u2} = 0.5699$ kg $\cdot$ m^2/s; $r_1 = r_3 = 0.02097\ \Omega$, $r_2 = 0.01591\ \Omega$; $l_1 = l_3 = 1.383 \times 10^{-3}$ H, $l_2 = 1.278 \times 10^{-3}$ H; $\eta_1 = \eta_3 = 1.807$, $\eta_2 = 1$; $B = 1.25$ m; $Ks_1 = Ks_3 = 108$, $Ks_2 = 135.1$; $K_1 = K_3 = 23.6749$ N $\cdot$ m/A, $K_2 = 32.6089$ N $\cdot$ m/A.

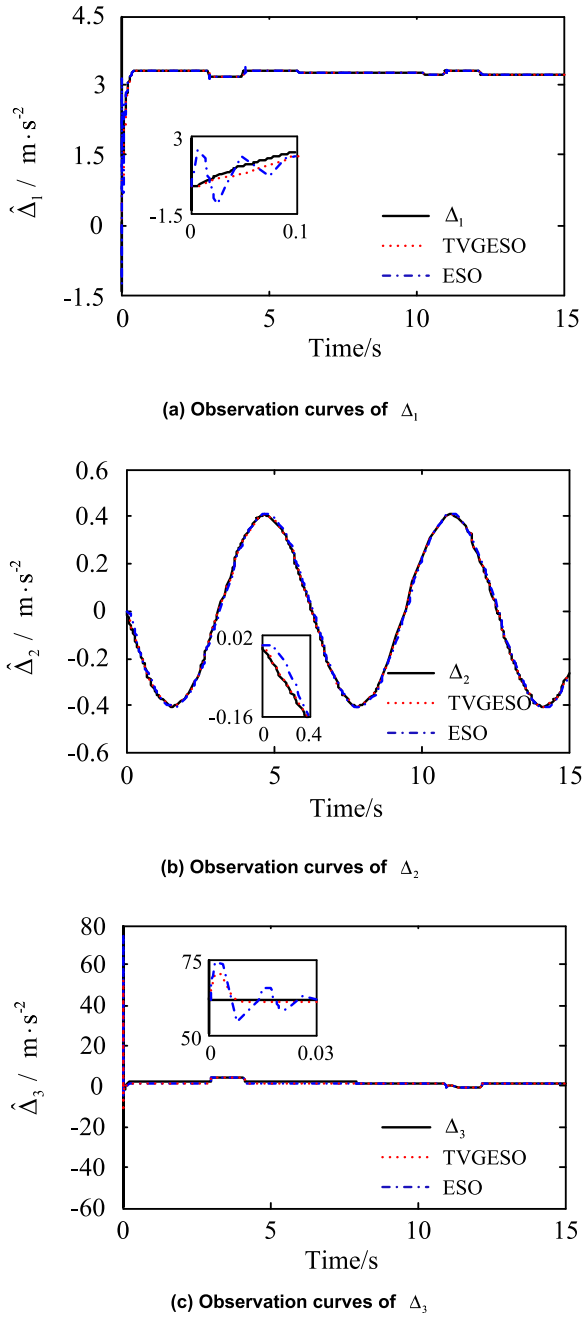

FIGURE 3. Observation curves of TVGESOs.

The main parameters of the proposed control strategy are chosen as $k_{11} = k_{31} = 10$, $k_{21} = 300$, $k_{12} = k_{32} = 5 \times 10^4$; $\tau_{11} = \tau_{12} = \tau_{21} = \tau_{22} = \tau_{31} = \tau_{32} = 0.001$, $\tau_{14} = \tau_{33} = \tau_{34} = 0.01$; $\gamma_{11} = \gamma_{12} = \gamma_{31} = \gamma_{32} = 1.5$, $\gamma_{21} = \gamma_{22} = 5$, $\gamma_{13} = \gamma_{14} = \gamma_{33} = \gamma_{34} = 2$; $k_{13\max} = 0.8$, $k_{13\min} = 0.3$, $k_{14\max} = 2$, $k_{14\min} = 1$, $k_{22\max} = k_{23\max} = 0.8$, $k_{22\min} = k_{23\min} = 0.5$, $k_{33\max} = 4$, $k_{33\min} = 2.5$, $k_{34\max} = 8$, $k_{34\min} = 1$; $\zeta_{13} = 1$, $\zeta_{14} = 2$, $\zeta_{22} = \zeta_{23} = 2$,

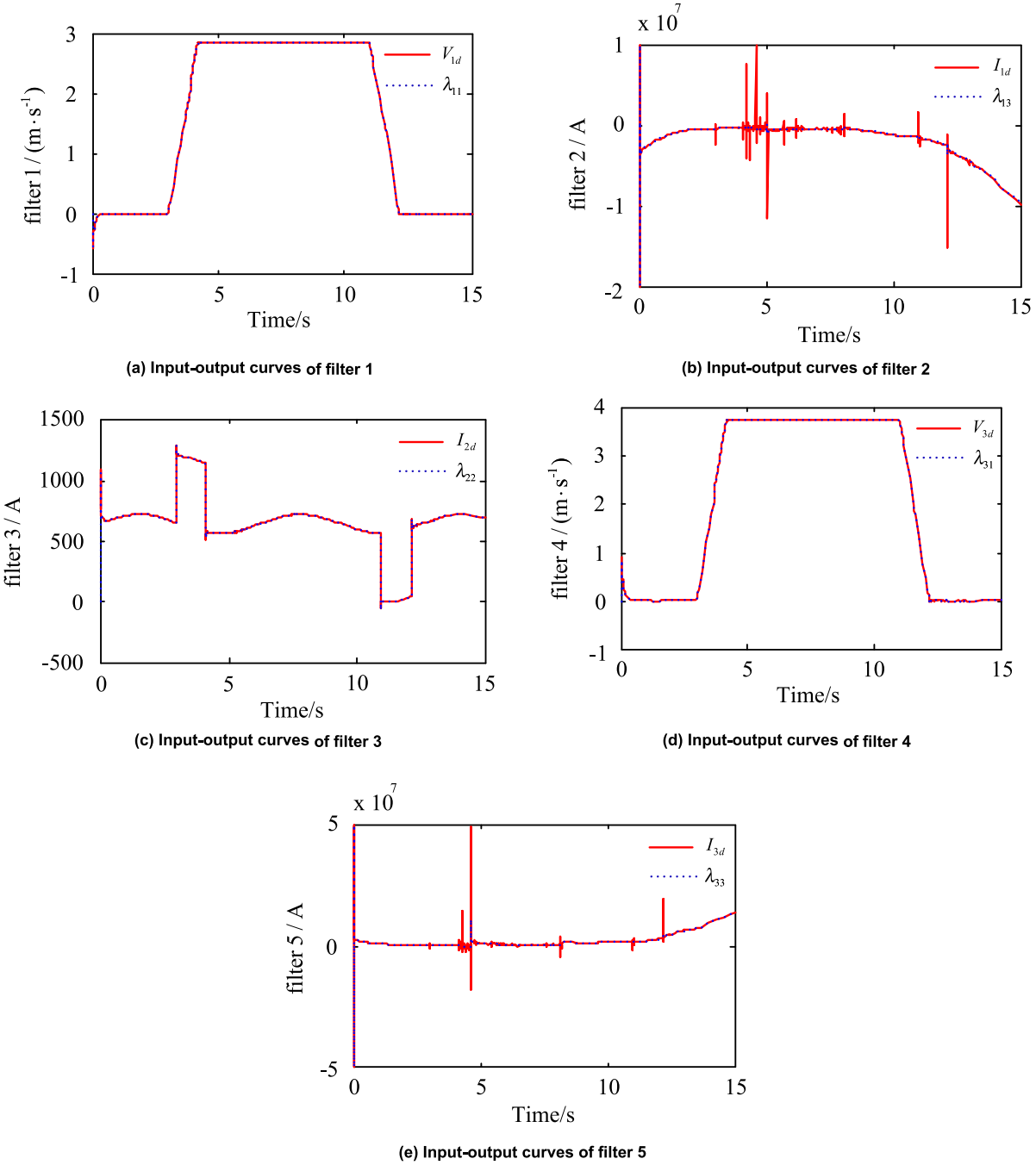

FIGURE 4. Input-output curves of second order integral filters.

$\zeta_{33} = 5$, $\zeta_{34} = 8$; $\phi_{13} = \phi_{14} = \phi_{33} = \phi_{34} = 0.01$, $\phi_{22} = \phi_{23} = 0.001$; $\vartheta_1 = \vartheta_2 = \vartheta_3 = 0.8$; $g_{21} = 3$, $g_{22} = 5$, $g_{11} = g_{12} = g_{31} = g_{32} = 1$.

Assume there exists parameter perturbations and load disturbance in the actual rolling process of the reversible cold strip rolling mill, that is, B_{ui} changes into 1.2 B_{ui}, r_i changes into 1.3 r_i, and the load disturbance is $\Delta M_z = 2500\sin(t)$ N · m.

Without loss of the generality, the rolling process of the reversible cold strip rolling mill for one pass is imitated: first, the left coiler tension rises to 100 KN and the right coiler tension rises to 120 KN within 0-3 s, so as to build strip steel tension on both sides of the main rolling mill; next, the main rolling mill speed rises to 3.5 m/s within 3-5 s, and starts the normal rolling process; at the time of $t = 11$ s, the main rolling mill speed reduces to 0 m/s gradually, and the rolling pass is over.

Remark 6: During the rolling process of the reversible cold strip rolling mill, in order to prevent the harmful impact on the system device due to the main rolling mill speed changing

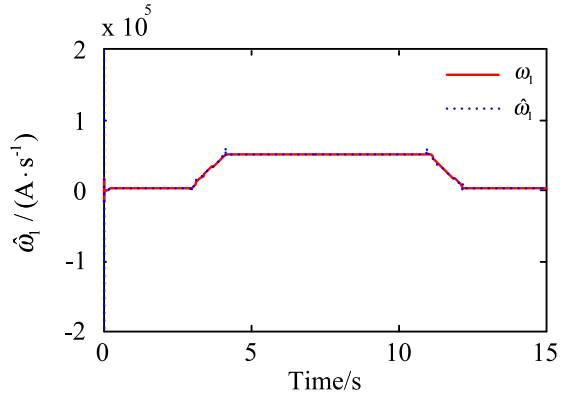

(a) Approximation curve of ω_1

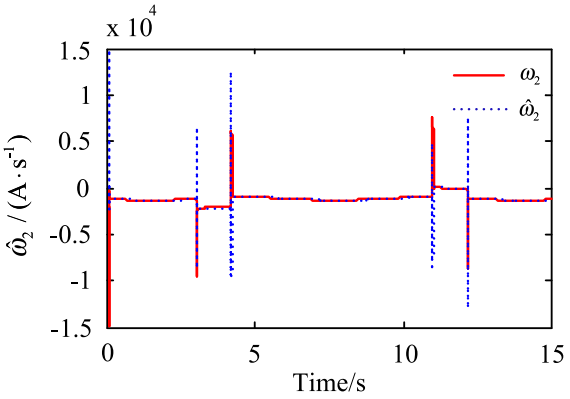

(b) Approximation curve of ω_2

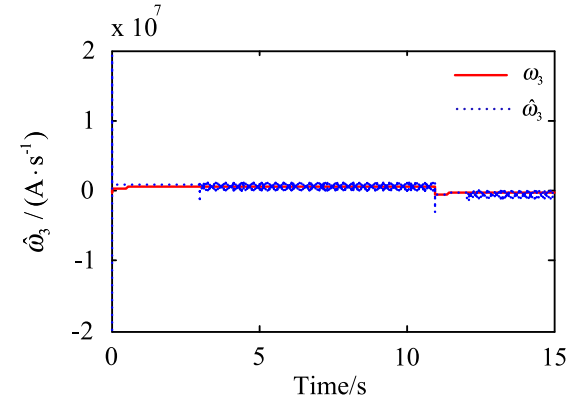

(c) Approximation curve of ω_3

FIGURE 5. Approximation curves of neural networks.

too quickly, the given slope for the main rolling mill speed is limited at $a_{\max,\min} = \pm 3$ m/s^2.

The coordinated tracking control response curves of the reversible cold strip rolling mill are shown as Fig. 2. As can be clearly seen in Fig. 2(a)-(c): 1) Under the action of the traditional NTSM control strategy, the system state variables F_1, V_2, and F_3 can realize the effective tracking controls for the given values F_1^*, V_2^*, and F_3^*, while their dynamic response speeds are relatively slow, the tracking precisions are relatively poor, and the robust stabilities are relatively weak; 2) under the action of the proposed control strategy, the system state variables F_1, V_2, and F_3 not only realize coordinated tracking controls, but also have faster dynamic response speeds, higher stability precisions and better anti-interference abilities. As can be clearly seen in Fig. 2(b), (d), and (e): 1) in the normal rolling stage, the main rolling mill speed is higher than the left coiler speed and lower than the right coiler speed, which helps to build strip steel tension on both sides of the main rolling mill, and then facilitates the smooth implementation of the rolling process; 2) under the action of the proposed control strategy, the dynamic responses of the left and right coilers are relatively faster, and the steady accuracies are relatively higher.

Observation curves of the TVGESOs are shown as Fig. 3. As can be clearly seen, both the designed TVGESOs and the traditional ESOs all realize effectively dynamic observations for the unmatched uncertainties (Δ_1, Δ_2, and Δ_3), which help to improve the control precision of the speed and tension system of the reversible cold strip rolling mill. In addition, under the actions of the designed TVGESOs, the initial peak phenomenon is effectively suppressed.

The input-output curves of the second order sliding mode integral filters are shown as Fig. 4. As can be clearly seen, the designed second order sliding mode integral filters realize effective estimations for the virtual control inputs during using the backstepping control, which avoid the ''differential explosion'' phenomena and simplify the calculation process of the designed controllers effectively.

Approximation curves of the neural networks are shown as Fig. 5. As can be clearly seen, the designed neural networks realize effectively dynamic approximations for the matched uncertainties (ω_1, ω_2, and ω_3), which can improve the control precision of the system.

VII. CONCLUSION

The coordinated tracking control problem for the speed and tension system of the reversible cold strip rolling mill has been investigated in this paper. First, the TVGESOs were constructed to counteract the unmatched uncertainties. Second, ANTSMCs were designed based on the backstepping control and the second order sliding mode integral filters, which not only avoided the ''differential explosion'' phenomena during using the backstepping control effectively, but also improved the robust stability of system. Third, the neural network adaptive method was used to approximate the matched uncertainties, which improved the coordinated tracking control precision of the system effectively. Theoretical analysis has shown that all signals in the closed-loop system are stable, and the sliding mode variables can converge to bounds in finite time. Finally, through comparison with the traditional NTSM backstepping control strategy based on ESO, simulation results illustrated that the speed and tension system can not only realize effective coordinated tracking control, but also has better dynamic and static performance, and anti-interference ability under the action of the proposed control strategy.

REFERENCES

[1] X. Ma, D. Wang, and H. Liu, "Coupling mechanism of control on strip profile and flatness in single stand universal crown reversible rolling mill," *Steel Res. Int.*, vol. 88, no. 9, Sep. 2017, Art. no. 1600495.

[2] G.-M. Liu, H.-S. Di, C.-L. Zhou, H.-C. Li, and J. Liu, "Tension and thickness control strategy analysis of two stands reversible cold rolling mill," *J. Iron Steel Res. Int.*, vol. 19, no. 10, pp. 20–25, Oct. 2012.

[3] X.-C. Wang, Q. Yang, Z.-Y. Jiang, and J. W. Xu, "Research on the improvement effect of high tension on flatness deviation in cold strip rolling," *Steel Res. Int.*, vol. 85, no. 11, pp. 1560–1570, Nov. 2015.

[4] K. Prinz, A. Steinboeck, M. Müller, A. Ettl, and A. Kugi, "Automatic gauge control under laterally asymmetric rolling conditions combined with feedforward," *IEEE Trans. Ind. Appl.*, vol. 53, no. 3, pp. 2560–2568, May 2017.

[5] J.-L. Sun, Y. Peng, and H.-M. Liu, "Dynamic characteristics of cold rolling mill and strip based on flatness and thickness control in rolling process," *J. Central South Univ.*, vol. 21, no. 2, pp. 567–576, Feb. 2014.

[6] L. Liu, Y. Fang, J. Li, and R. Chang, "Modeling and decentralized control for speed and tension multivariable coupling system of reversible cold strip mill," *Control Theory Appl.*, vol. 31, no. 1, pp. 42–48, Jan. 2014.

[7] J. Yao, Z. Jiao, D. Ma, and L. Yan, "High-accuracy tracking control of hydraulic rotary actuators with modeling uncertainties," *IEEE/ASME Trans. Mechatronics*, vol. 19, no. 2, pp. 633–641, Apr. 2014.

[8] J. Yao, Z. Jiao, and D. Ma, "RISE-based precision motion control of DC motors with continuous friction compensation," *IEEE Trans. Ind. Electron.*, vol. 61, no. 12, pp. 7067–7075, Dec. 2014.

[9] Z. Yao, J. Yao, and W. Sun, "Adaptive RISE control of hydraulic systems with multilayer neural-networks," *IEEE Trans. Ind. Electron.*, vol. 66, no. 11, pp. 8638–8647, Nov. 2019.

[10] L.-X. Liu, Y.-M. Fang, J.-X. Li, and D.-S. Li, "Decentralized overlapping control for speed and tension in reversing cold-strip mill," (in Chinese), *Control Theory Appl.*, vol. 28, no. 5, pp. 675–680, 2011.

[11] R. Bai, S. C. Tong, and T. Y. Chai, "Modeling and decoupling control for the strip tension of bridling roll in the continuous annealing line," *Control Theory Appl.*, vol. 30, no. 3, pp. 392–397, Mar. 2013.

[12] Y. Fang, L. Liu, J. Li, and Y. Xu, "Decoupling control based on terminal sliding mode and wavelet network for the speed and tension system of reversible cold strip rolling mill," *Int. J. Control*, vol. 88, no. 8, pp. 1630–1646, Aug. 2015.

[13] H. Koc, D. Knittel, M. de Mathelin, and G. Abba, "Modeling and robust control of winding systems for elastic webs," *IEEE Trans. Control Syst. Technol.*, vol. 10, no. 2, pp. 197–208, Mar. 2002.

[14] Y.-M. Fang, L. Liu, J.-M. Li, and R. Chang, "Compound control for speed and tension multivariable coupling system of reversible cold strip mill," *J. Central South Univ.*, vol. 22, no. 2, pp. 529–538, Feb. 2015.

[15] M. Chen, S.-Y. Shao, and B. Jiang, "Adaptive neural control of uncertain nonlinear systems using disturbance observer," *IEEE Trans. Cybern.*, vol. 47, no. 10, pp. 3110–3123, Oct. 2017.

[16] Q. Zhang, Q.-X. Wu, C.-S. Jiang, and Y.-H. Wang, "Robust reconfigurable tracking control of near space vehicle with actuator dynamic and input constraints," *Control Theory Appl.*, vol. 29, no. 10, pp. 1263–1271, Oct. 2012.

[17] X.-D. Lu, H. Zhao, B. Zhao, and J. Zhou, "Disturbance compensation-based integrated guidance and control design for near space interceptor," *Control Decis.*, vol. 32, no. 10, pp. 1782–1788, 2017.

[18] Y. Wang, J. Chen, K. Zhu, B. Chen, and H. Wu, "Time-delay control of cable-driven robots with adaptive fractional-order nonsingular terminal sliding mode," *IEEE Access*, vol. 6, pp. 54086–54096, Sep. 2018.

[19] L. Zhang, Z. Li, and C. Yang, "Adaptive neural network based variable stiffness control of uncertain robotic systems using disturbance observer," *IEEE Trans. Ind. Electron.*, vol. 64, no. 3, pp. 2236–2245, Mar. 2017.

[20] Z.-L. Tang, S. S. Ge, K. P. Tee, and W. He, "Robust adaptive neural tracking control for a class of perturbed uncertain nonlinear systems with state constraints," *IEEE Trans. Syst., Man, Cybern. Syst.*, vol. 46, no. 12, pp. 1618–1629, Dec. 2016.

[21] M. Chen and S. S. Ge, "Adaptive neural output feedback control of uncertain nonlinear systems with unknown hysteresis using disturbance observer," *IEEE Trans. Ind. Electron.*, vol. 62, no. 12, pp. 7706–7716, Dec. 2015.

[22] C.-Y. Chen, Y. Tang, L.-H. Wu, M. Lu, X.-S. Zhan, X. Li, C.-L. Huang, and W.-H. Gui, "Adaptive neural-network-based control for a class of nonlinear systems with unknown output disturbance and time delays," *IEEE Access*, vol. 7, pp. 7702–7716, 2019.

[23] L. Liu, Y. Han, Y. Fang, M. Lin, and N. Shao, "Neural network dynamic surface backstepping control for the speed and tension system of reversible cold strip rolling mill," *Asian J. Control*, vol. 20, no. 4, pp. 1452–1463, Jul. 2018.

[24] R. Zhang, L. Dong, and C. Sun, "Adaptive nonsingular terminal sliding mode control design for near space hypersonic vehicles," *IEEE/CAA J. Autom. Sinica*, vol. 1, no. 2, pp. 155–161, Apr. 2014.

[25] J. Zheng, H. Wang, Z. Man, J. Jin, and M. Fu, "Robust motion control of a linear motor positioner using fast nonsingular terminal sliding mode," *IEEE/ASME Trans. Mechatronics*, vol. 20, no. 4, pp. 1743–1752, Aug. 2015.

[26] H. Wang, L. Shi, Z. Man, J. Zheng, S. Li, M. Yu, C. Jiang, H. Kong, and Z. Cao, "Continuous fast nonsingular terminal sliding mode control of automotive electronic throttle systems using finite-time exact observer," *IEEE Trans. Ind. Electron.*, vol. 65, no. 9, pp. 7160–7172, Sep. 2018.

[27] C.-F. Chen, Z.-J. Du, L. He, J.-Q. Wang, D.-M. Wu, and W. Dong, "Active disturbance rejection with fast terminal sliding mode control for a lower limb exoskeleton in swing phase," *IEEE Access*, vol. 7, pp. 72343–72357, 2019.

[28] M. Jin, J. Lee, and K. K. Ahn, "Continuous nonsingular terminal sliding-mode control of shape memory alloy actuators using time delay estimation," *IEEE/ASME Trans. Mechatronics*, vol. 20, no. 2, pp. 899–909, Apr. 2015.

LE LIU received the B.E. degree in automation from the Hebei University of Science and Technology, in 2008, and the M.E. and Ph.D. degrees in control science and engineering from Yanshan University, China, in 2011 and 2015, respectively. He is currently an Associate Professor with the Department of Automation, Yanshan University. His research interests include decoupling coordinated control of multivariable systems, robust control, and its applications to nonlinear systems.

SUYAN DING is currently pursuing the master's degree with the Department of Automation, Yanshan University, China. Her research interests include coordinated control for the speed and tension system of cold strip rolling mill.

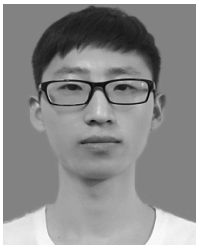

JIE GAO is currently pursuing the master's degree with the Department of Automation, Yanshan University, China. His research interests include AC asynchronous motor tracking control.

YIMING FANG received the B.E. and M.E. degrees in automation from the Northeast Heavy Machinery Institute (which was renamed Yanshan University in 1997), China, in 1985 and 1988, respectively, and the Ph.D. degree in mechanical and electronic engineering from Yanshan University, China, in 2003. He is currently a Professor with the Department of Automation, Yanshan University. His research interests include modeling and simulation and control of complex systems, as well as adaptive robust control of metallurgical automation systems.